

# Comparison of Galerkin Finite Element, Modified Method of Characteristics and Random Walk Models for Solute Transport Simulation in Groundwater Flow Systems

*N.H.Kulkarni and A.K.Rastogi*

**Abstract**— This paper compares Galerkin finite element (FE-SOLUTE), Modified Method of Characteristics (MMOC-SOLUTE) and Random Walk (RWSOLUTE) models for the simulation of solute transport in two-dimensional, transient, unconfined groundwater flow systems. This study involves validation of these models by comparing the model results with the reported solutions of the model presented by N-Z Sun. (1996). These models are further used to obtain the space and time distribution of head and concentration for the reported synthetic test case. The effect of time step size and space discretizations is analyzed on model results using Peclet and Courant numbers. Based on numerical oscillations and dispersion the best performing model amongst these models is decided to simulate solute transport in groundwater flow systems.

**Keywords**—Solute transport models, Unconfined groundwater flow, , Space time distribution of concentration, Validation of numerical solute transport models

## I. INTRODUCTION

Groundwater quality deterioration in many parts of the world due to poorly planned municipal, agricultural and industrial waste disposal practices has drawn the attention of researchers to develop new methods of predicting and analyzing the impact of the migration of the dissolved solutes reliably in the aquifers. The pollution of this vital water resource resulted into a serious environmental problem which may damage human health, destroy the ecosystem and cause water shortage. Thus it has become essential to assess the severity of groundwater pollution and chalk out the strategies of aquifer remediation, which are made possible by the use of the numerical models. The groundwater pollution problem becomes severe because of the migration of solutes by advection and hydrodynamic dispersion from the point of its introduction in aquifers [Freeze and Cherry, 1979].

Numerical models of groundwater flow and solute transport are properly conceptualized version of a complex aquifer system which approximates the flow and transport phenomena. The approximations in the numerical models are effected in through the set of assumptions pertaining to the geometry of the domain, ways the heterogeneities are smoothed out, the nature of the porous medium, properties of the fluid and the type of the flow regime. The complex aquifer system is treated as a continuum, which implies that the fluid and solid matrix variables are continuously defined at every point in the aquifer domain. The continuum is viewed as a network of several representative elementary volumes, each representing a portion of the entire volume of an aquifer with average fluid and solid properties taken over it and assigned to the nodes of superimposed grid used for the discretization of the domain.

Numerical models are applied either in an interpretive sense to gain insight into controlling the aquifer parameters in a site-specific setting or in generic sense to formulate regional regulatory guidelines and act as screening tools to identify regions suitable for some proposed action e.g. artificial recharge and aquifer remediation.

Bredehoeft and Pinder (1973) developed the Galerkin finite element model for the solution of the solute mass transport equation. This model is used to predict the future movement of conservative solute in the groundwater system. They implemented the developed numerical model for chosen field study. The average solute mass flux is interpolated from the groundwater flow equation.

Smith et al. (1973) approximated the dispersive part of the advection-dispersion equation by Galerkin finite element method. The paper discusses the accuracy and stability of Galerkin finite element method in relation to numerical dispersion phenomena. It has been shown that the developed model can efficiently model the dispersive phenomenon.

Neuman et al. (1984) proposed a new adaptive Eulerian-Lagrangian formulation for the solution of the advective – dispersion equation. In this method the advective component of steep concentration front is tracked forward with the aid of moving particles clustered around each front and away from such fronts the advective transport is simulated by single step reverse particle tracking and when a front dissipates with time the forward tracking stops automatically and the

---

N.H.Kulkarni is working as Associate Professor, Dept. of Civil & Water Management Engg., SGGSI&T,Nanded- 431 606. and A.K.Rastogi is working as Professor, Dept. of Civil Engg., IIT Bombay- 400076.

corresponding cloud of particles is eliminated. The dispersion problem is solved by Lagrangian formulation on a fixed grid. It is found from the results that this method is capable of handling the entire range of Peclet numbers from zero to infinity with courant numbers well in excess of unity.

Sorek et al. (1988) used a mixed Eulerian-Lagrangian method, which decomposes the equation into pure advection and residual dispersion. The governing equation is decomposed into advection along the characteristic path lines and the propagation of the solute mass residue at a fixed grid point. It is also reported that the simulation of solute transport by this method with coarse grid and high Peclet numbers yielded minute mass balance errors. The method is found to be efficient when it is implemented on a confined grid size with Peclet number less than or equal to 2.

Illangasekare et al. (1989) developed a simulation model of two-dimensional solute transport in water table aquifers. They used discrete kernel approach for solving the linear governing partial differential equation of groundwater flow. The solution of the flow equation gives the flow velocities resulting from different pumping and injection schemes. The flow model is validated against analytical solutions. A method of characteristic simulation model was developed to simulate the two-dimensional transient solute transport in water table aquifers. The proposed model is implemented for various test cases and it is found that the computed solute concentration breakthrough curves closely match the breakthrough curves obtained by analytical solutions.

Uffink et al. (1988) presented a random walk solute transport model that is different than the conventional model. The random walk is used as a mathematical concept to create an analogue process that obeys the classical advection-dispersion equation. The paper also discusses the conditions required for a complete equivalency between random walk and advection-dispersion equation. It proposes the use of proper coefficients in Fokker-Plank equation to eliminate the occurrence of unphysical high solute concentrations due to trapping of particles near stagnation points or in the parts of the aquifer with a much lower permeability than the surrounding area.

Wen et al. (1996) proposed a constant displacement scheme of particle tracking for simulation of advective transport. This scheme automatically adjusts the time step for each particle according to local pore velocity so that each particle always travels a constant distance. The application of this scheme for two-dimensional solute transport in groundwater flow system is found to be four times computationally faster than constant time step scheme which is conventionally used in particle tracking in random walk model simulations.

## II. GROUNDWATER FLOW EQUATION

The governing equation of two-dimensional, horizontal, and transient groundwater flow in homogeneous, isotropic and unconfined aquifer is given as [ 8]

$$S_y \frac{\partial h}{\partial t} = T_{xx} \frac{\partial^2 h}{\partial x^2} + T_{yy} \frac{\partial^2 h}{\partial y^2} + \sum_{i=1}^{n_w} Q_i \delta(x_o - x_i, y_o - y_i) + \sum_{j=1}^{n_p} q_j \quad (1)$$

where  $S_y$  is the specific yield, [dimensionless];  $h$  is the hydraulic head averaged over vertical, [  $L$  ];  $t$  is the time, [  $T$  ];  $T_{xx}$  and  $T_{yy}$  are components of the transmissivity tensor, [  $L^2/T$  ] which are approximated as  $T_{xx} \approx K_{xx} h$  and  $T_{yy} \approx K_{yy} h$ , provided the change in the head in unconfined aquifer is negligible as compared to its saturated thickness [8];  $K_{xx}$  and  $K_{yy}$  are components of the hydraulic conductivity tensor, [  $L/T$  ];  $x$  and  $y$  are spatial coordinates, [  $L$  ];  $Q_i$  is the pumping rate when ( $Q_i < 0$ ) and injection rate when ( $Q_i > 0$ ) at  $i$  th pumping and / or injection well, [  $L^3/T$  ];  $n_w$  is the number of pumping and/or injection wells in the domain;  $n_p$  is the number of nodes in the domain with distributed discharge and/or recharge;  $\delta(x_o - x_i, y_o - y_i)$  is the Dirac delta function;  $x_o$  and  $y_o$  are the Cartesian coordinates of the origin, [  $L$  ];  $x_i$  and  $y_i$  are the coordinates of  $i$  th pumping and / or injection well, [  $L$  ];  $q_j$  is the distributed discharge rate when ( $q_j < 0$ ) and recharge rate when ( $q_j > 0$ ) at  $j$  th nodes with distributed discharge and/or recharge, [  $L/T$  ].

Equation (1) is subject to the following initial condition which is given as

$$h(x, y, 0) = h_0 \quad (x, y) \in \Omega \quad (2)$$

where  $h_0$  is the initial head over the entire flow domain, [  $L$  ] and  $\Omega$  is the flow domain, [  $L^2$  ]. Equation (1) is subject to the Dirichlet type of boundary condition which is given as

$$h(x, y, t) = h_1 \quad (x, y) \in \Gamma_1; t \geq 0 \quad (3)$$

where  $h_1$  is the prescribed head over aquifer domain boundary  $\Gamma_1$ , [  $L$  ]. The Neumann boundary condition with zero groundwater flux can be given as

$$\{[q_b(x, y, t)] - [T] \nabla h(x, y, t)\} \cdot \{n\} = 0 \quad (x, y) \in \Gamma_2; t \geq 0 \quad (4)$$

where  $q_b$  is the specified groundwater flux across boundary  $\Gamma_2$ , [  $L/T$  ];  $[T] \nabla h$  is the groundwater flux across the boundary  $\Gamma_2$ , [  $L/T$  ] and  $n$  is normal unit vector in outward direction.

## III. ADVECTION-DISPERSION EQUATION

The governing equation of solute transport in two-dimensional transient unconfined groundwater flow system referred to as advection-dispersion equation is given as [8].

$$R \frac{\partial c}{\partial t} = D_{xx} \frac{\partial^2 c}{\partial x^2} + D_{xy} \frac{\partial^2 c}{\partial x \partial y} + D_{yx} \frac{\partial^2 c}{\partial y \partial x} + D_{yy} \frac{\partial^2 c}{\partial y^2} - V_x \frac{\partial c}{\partial x} - V_y \frac{\partial c}{\partial y} + \sum_{i=1}^{n_w} \frac{(c - c_i)}{\theta b} Q_i \delta(x_o - x_i, y_o - y_i) + \sum_{j=1}^{n_p} \frac{q_j}{\theta} (c - c_j) + \frac{c S_y}{\theta b} \frac{\partial h}{\partial t} \quad (5)$$

where  $R$  is the retardation factor, [dimensionless];  $c$  is solute concentration,  $[M/L^3]$ ;  $D_{xx}$ ,  $D_{xy}$ ,  $D_{yx}$ , and  $D_{yy}$  are hydrodynamic dispersion coefficients,  $[L^2/T]$ ;  $V_x$  and  $V_y$  are the components of average linear groundwater velocity,  $[L/T]$ ;  $c_i$  is solute concentration of the injected water at  $i$ th injection well,  $[M/L^3]$ ;  $n_w$  is the number of injection wells in the domain;  $\theta$  is the effective porosity of the aquifer, [percent];  $b$  is the saturated thickness of the aquifer,  $[L]$ ;  $c_j$  is solute concentration of the recharge water at  $j$ th node with distributed recharge,  $[M/L^3]$  and  $n_p$  is the number of nodes with distributed recharge .

Equation (5) is subject to the following initial condition which is given as

$$c(x, y, 0) = c_0 \quad (x, y) \in \Omega \quad (6)$$

where  $c_0$  is the initial solute concentration over the entire aquifer domain,  $[M/L^3]$ .

Equation (5) is subject to the Dirichlet boundary condition which is given as

$$c(x, y, t) = c_1 \quad (x, y) \in \Gamma_1; t \geq 0 \quad (7)$$

where  $c_1$  is the prescribed solute concentration over aquifer domain boundary  $\Gamma_1$ ,  $[M/L^3]$ .

Equation (5) is subject to the Neumann boundary condition which is given as

$$[cq_b(x, y, t) - [D]\nabla c(x, y, t)] \cdot \hat{n} = 0 \quad (x, y) \in \Gamma_2; t \geq 0 \quad (8)$$

where  $cq_b$  is the specified solute flux across the boundary  $\Gamma_2$ ,  $[M/L^3/T]$  and  $[D]\nabla c$  is the dispersive flux across the boundary  $\Gamma_2$ ,  $[M/L^3/T]$ .

#### IV. FESOLUTE MODEL

Applying the numerical integration for the various terms of Equation (5) the following system of linear equations is obtained and the same can be written as

$$\left( [A] + \frac{1}{\Delta t} [B] \right) \{c_L^{t+\Delta t}\} = \left( \frac{1}{\Delta t} [B] \right) \{c_L^t\} + \{d_L\} + \{g_L\} \quad (9)$$

where  $[A]$  is the global conductance matrix which is formed by assembling the elemental conductance matrices  $[A_L^e]$  that can be expressed as

$$A_L^e = \iint_e \left( D_{xx} \frac{\partial \hat{c}_L^e}{\partial x} \frac{\partial N_L^e}{\partial x} + D_{xy} \frac{\partial \hat{c}_L^e}{\partial y} \frac{\partial N_L^e}{\partial x} + D_{yx} \frac{\partial \hat{c}_L^e}{\partial x} \frac{\partial N_L^e}{\partial y} + D_{yy} \frac{\partial \hat{c}_L^e}{\partial y} \frac{\partial N_L^e}{\partial y} \right) dx dy - \iint_e \left( V_x \hat{c}_L^e \frac{\partial N_L^e}{\partial x} + V_y \hat{c}_L^e \frac{\partial N_L^e}{\partial y} \right) dx dy = \frac{D_{xx}}{4A^e} \begin{bmatrix} b_i^e b_i^e & b_i^e b_j^e & b_i^e b_k^e \\ b_j^e b_i^e & b_j^e b_j^e & b_j^e b_k^e \\ b_k^e b_i^e & b_k^e b_j^e & b_k^e b_k^e \end{bmatrix} + \frac{D_{xy}}{4A^e} \begin{bmatrix} b_i^e c_i^e & b_i^e c_j^e & b_i^e c_k^e \\ b_j^e c_i^e & b_j^e c_j^e & b_j^e c_k^e \\ b_k^e c_i^e & b_k^e c_j^e & b_k^e c_k^e \end{bmatrix} + \frac{D_{yx}}{4A^e} \begin{bmatrix} c_i^e b_i^e & c_i^e b_j^e & c_i^e b_k^e \\ c_j^e b_i^e & c_j^e b_j^e & c_j^e b_k^e \\ c_k^e b_i^e & c_k^e b_j^e & c_k^e b_k^e \end{bmatrix} + \frac{D_{yy}}{4A^e} \begin{bmatrix} c_i^e c_i^e & c_i^e c_j^e & c_i^e c_k^e \\ c_j^e c_i^e & c_j^e c_j^e & c_j^e c_k^e \\ c_k^e c_i^e & c_k^e c_j^e & c_k^e c_k^e \end{bmatrix} + \frac{V_x^e}{6} \begin{bmatrix} b_i^e \\ b_j^e \\ b_k^e \end{bmatrix} - \frac{V_y^e}{6} \begin{bmatrix} c_i^e \\ c_j^e \\ c_k^e \end{bmatrix} \quad (10)$$

$[B]$  is the global storage matrix which is assembled from elemental storage matrices  $[B_L^e]$  that can be given as

$$B_L^e = \iint_e R^e \frac{\partial \hat{c}_L^e}{\partial t} N_L^e dx dy = \iint_e R^e N_L^e N_L^e dx dy = R^e \frac{A^e}{12} \begin{bmatrix} 2 & 1 & 1 \\ 1 & 2 & 1 \\ 1 & 1 & 2 \end{bmatrix} \quad L = i \neq j \neq k \quad (11)$$

$\{d_L\}$  is the global load vector which is assembled from elemental load vectors  $\{d_L^e\}$  that can be given as

$$d_L^e = \iint_e \left( \sum_{i=1}^{n_w} (\hat{c}_L^e - c_i^e) Q_i^e \delta(x_o - x_i^e, y_o - y_i^e) + \sum_{j=1}^{n_p} (\hat{c}_L^e - c_j^e) q_j^e + \left( \frac{\hat{c}_L^e S_{yL}^e}{T^e} \frac{\partial h_L^e}{\partial t} \right) \right) N_L^e dx dy = \frac{dx}{dt} = V_x, \frac{dy}{dt} = V_y \frac{dc}{dt} = \frac{\partial c}{\partial t} + \frac{dx}{dt} \frac{\partial c}{\partial x} + \frac{dy}{dt} \frac{\partial c}{\partial y} \quad (15)$$

$$\left( (\hat{c}_L^e - c_i^e) Q_i^e \delta(x_o - x_i^e, y_o - y_i^e) \frac{1}{3} + \sum_{j=1}^{n_p} (\hat{c}_L^e - c_j^e) q_j^e \frac{A^e}{3} + \left( \frac{\hat{c}_L^e S_{yL}^e}{T^e} \frac{(h_L^{t+\Delta t} - h_L^t)}{\Delta t} \right) \frac{A^e}{3} \right) \begin{bmatrix} 1 \\ 1 \\ 1 \end{bmatrix} \quad (12)$$

Thus the location of the base of the characteristic curve which represents the probable location of the drifting particle at the previous time level from which it has come to the nodal location during a time step is obtained by using following equations:

$$\delta x_{i,j}^t = V_{x_{i,j}} \times \Delta t, \delta y_{i,j}^t = V_{y_{i,j}} \times \Delta t \quad (16)$$

{g} is the global boundary flux vector which is assembled from the elemental boundary flux vectors {g<sub>L</sub><sup>e</sup>} that can be given as

$$g_L^e = \int_e \left( D_{xx} \frac{\partial \hat{c}_L^e}{\partial x} n_x + D_{yy} \frac{\partial \hat{c}_L^e}{\partial y} n_y \right) N_L^e d\sigma = \left( c_L^e \frac{q_{bx}^e}{L} \frac{d\sigma^e}{2} + c_L^e \frac{q_{by}^e}{L} \frac{d\sigma^e}{2} \right) \begin{bmatrix} 1 \\ 1 \\ 1 \end{bmatrix} \quad (13)$$

From the known concentration distribution at previous time level the unknown concentration distribution at the next time level is obtained by recursively solving the set of algebraic equations given in Equation (9).

**V. MMOC SOLUTE MODEL**

This model is proposed as a variant of the conventional USGS-MOC model. Unlike the conventional USGS-MOC model, real solute particles are used for the simulation of the advective transport. Each solute particle has definite volume which is equal to the volume of the cell accommodating that particle and it drifts through the groundwater flow system due to the average linear groundwater velocity. The second order hydrodynamic dispersion term is handled by finite element method.

This model considers the Equation (5) in its material derivative form so as to replace the hyperbolic form of equation due to advection terms with the parabolic form of equation containing hydrodynamic dispersion terms and discharge and/or recharge terms and the same is given as

$$\frac{Dc}{Dt} \equiv \left( \frac{\partial c}{\partial t} + V_x \frac{\partial c}{\partial x} + V_y \frac{\partial c}{\partial y} \right) = D_{xx} \frac{\partial^2 c}{\partial x^2} + D_{xy} \frac{\partial^2 c}{\partial x \partial y} + D_{yx} \frac{\partial^2 c}{\partial y \partial x} + D_{yy} \frac{\partial^2 c}{\partial y^2} + \sum_{i=1}^{n_w} \frac{Q_i (c - c_i)}{\theta b} + \sum_{j=1}^{n_p} \frac{q_j (c - c_j)}{\theta} + \frac{c S_y}{\theta b} \frac{\partial h}{\partial t} \quad (14)$$

The advection term of the Equation (9) is solved separately using backward in time particle tracking along characteristic curves. The solution of the advection term is the solution of the equations of characteristic curves which are given as

where δx<sub>i,j</sub><sup>t</sup> and δy<sub>i,j</sub><sup>t</sup> are the advective displacements in x- and y-directions, respectively. For the particle residing in third quadrant after advective transport, the concentration at the drifted location of the solute particle which happens to be the base of the characteristic curve is computed by using following equation:

$$c_{i,j}^{t+\Delta t} = c_R^t = (1 - f_y) \{ (1 - f_x) (c_{i,j}^t) + (f_x) (c_{i-1,j}^t) \} + (f_y) \{ (1 - f_x) (c_{i,j-1}^t) + (f_x) (c_{i-1,j-1}^t) \} \quad (17)$$

where c<sub>i,j</sub><sup>t+Δt</sup> is the concentration at the node after advective movement which is same as that of the concentration at the base of the characteristic curve i.e. c<sub>R</sub><sup>t</sup>, [M / L<sup>3</sup>]; R is the location of the base of the characteristic curve; f<sub>x</sub> = (Δx - δx<sub>i,j</sub><sup>t</sup>) / Δx and f<sub>y</sub> = (Δy - δy<sub>i,j</sub><sup>t</sup>) / Δy are factors of bilinear interpolation; (i - 1, j; i - 1, j - 1; i, j - 1; i, j) are the indices of the closest nodes to the drifted location of the particle. The change in nodal concentration at next time level i.e. c<sub>i,j</sub><sup>t+Δt</sup> is computed by approximating the second-order hydrodynamic dispersion term.

$$A_L^e = \iint_e \left( D_{xx} \frac{\partial \hat{c}_L^e}{\partial x} \frac{\partial N_L^e}{\partial x} + D_{xy} \frac{\partial \hat{c}_L^e}{\partial y} \frac{\partial N_L^e}{\partial x} + D_{yx} \frac{\partial \hat{c}_L^e}{\partial x} \frac{\partial N_L^e}{\partial y} + D_{yy} \frac{\partial \hat{c}_L^e}{\partial y} \frac{\partial N_L^e}{\partial y} \right) dx dy = \frac{D_{xx}}{4A^e} \begin{bmatrix} b_i^e b_i^e & b_i^e b_j^e & b_i^e b_k^e \\ b_j^e b_i^e & b_j^e b_j^e & b_j^e b_k^e \\ b_k^e b_i^e & b_k^e b_j^e & b_k^e b_k^e \end{bmatrix} + \frac{D_{xy}}{4A^e} \begin{bmatrix} b_i^e c_i^e & b_i^e c_j^e & b_i^e c_k^e \\ b_j^e c_i^e & b_j^e c_j^e & b_j^e c_k^e \\ b_k^e c_i^e & b_k^e c_j^e & b_k^e c_k^e \end{bmatrix} + \frac{D_{yx}}{4A^e} \begin{bmatrix} c_i^e b_i^e & c_i^e b_j^e & c_i^e b_k^e \\ c_j^e b_i^e & c_j^e b_j^e & c_j^e b_k^e \\ c_k^e b_i^e & c_k^e b_j^e & c_k^e b_k^e \end{bmatrix} + \frac{D_{yy}}{4A^e} \begin{bmatrix} c_i^e c_i^e & c_i^e c_j^e & c_i^e c_k^e \\ c_j^e c_i^e & c_j^e c_j^e & c_j^e c_k^e \\ c_k^e c_i^e & c_k^e c_j^e & c_k^e c_k^e \end{bmatrix} \quad (18)$$

Thus the changed nodal concentration after advective and dispersive transport is given as

$$c_{i,j}^{t+\Delta t} = c_{i,j}^{t+\Delta t} + c_{i,j}^{d,t+\Delta t} \quad (19)$$

### VI. RWSOLUTE MODEL

This model does not directly solve the Equation (5) rather it decouples that equation into advection and dispersion parts. The advective and dispersive transport of the solute mass is simulated with the help of particles. Each particle represents the fraction of the total solute mass in the aquifer system. The number of particles in a computational cell is worked out as

$$N_{i,j}^p = \frac{c_{i,j}^t(\theta \times \Delta x \times \Delta y \times b) + c_{i,j}^t((Q_{i,j} \delta(x_0 - x_i, y_0 - y_j)) + q_{i,j})(\theta \times \Delta x \times \Delta y \times b)}{PM} \quad (20)$$

The advective displacement components of the particle in x- and y-direction during a given time step due to average linear groundwater flow velocity can be given as

$$dx_p^a = V_{x_p} \times \Delta t \quad dy_p^a = V_{y_p} \times \Delta t \quad (21)$$

where  $dx_p^a, dy_p^a$  are the advective displacement components of  $p$  the particle during a time step  $\Delta t$ .

The dispersive transport of the particle due to hydrodynamic dispersion is calculated from the random movement of particles following the Gaussian normal distribution. The dispersive transport of a particle in x- and y-direction during a given time step can be given as

$$\begin{aligned} dx_p^d &= Z_{L_p} \sin \phi + Z_{T_p} \cos \phi = Z_{L_p} \frac{dx_p^a}{dl_1^a} + Z_{T_p} \frac{dy_p^a}{dl_1^a} \\ dy_p^d &= Z_{L_p} \cos \phi - Z_{T_p} \sin \phi = Z_{L_p} \frac{dy_p^a}{dl_1^a} - Z_{T_p} \frac{dx_p^a}{dl_1^a} \end{aligned} \quad (22)$$

where  $dx_p^d, dy_p^d$  are the dispersive transport components of  $p$  th particle during  $\Delta t$ ,  $[L]$ ;  $Z_{L_p} = N(0, \sigma_L^2)$  &  $Z_{T_p} = N(0, \sigma_T^2)$  are random numbers;  $N(0, \sigma_L^2)$  &  $N(0, \sigma_T^2)$  are normally distributed random numbers with zero mean and one standard deviation and which range from -6 to +6. Thus the total displacement of a particle in x- and y-direction during a given time step can be given as

$$x_p^{t+\Delta t} = x_p^t + dx_p^a + dx_p^d \quad y_p^{t+\Delta t} = y_p^t + dy_p^a + dy_p^d \quad (23)$$

where  $x_p^{t+\Delta t}, y_p^{t+\Delta t}$  is location of the  $p$  th particle at  $t + \Delta t$  time level, and  $x_p^t, y_p^t$  is the initial location of  $p$  th particle.

This procedure is repeated for all the particles generated in the cell. The change in nodal solute concentration during a time step is given as

$$c_{i,j}^{t+\Delta t} = c_{i,j}^t + (N_{i,j}^{t+\Delta t})PM \quad (24)$$

where  $N_{i,j}^{t+\Delta t}$  is the updated number of the particles residing in the computational cell after both advective and dispersive transport.

### VII. RESULTS AND DISCUSSION

Figure 1 shows the schematic of aquifer modeled in Test Case , [9]. This test case is aimed at validating FESOLUTE, RWSOLUTE and MMOC SOLUTE models. The aquifer is 80 m long and 70 m wide. The left and right sides of the aquifer are subject to no flow boundary conditions while the top and bottom sides are subject to prescribed head boundary conditions with the constant head of 100 m. The boundary conditions for solute transport simulation involve zero solute flux boundaries across the left and right sides and a concentration of 1 ppm on the bottom side and zero concentration at the top side of the aquifer. The groundwater is flowing in y-direction from south to north direction at the uniform velocity of 1.0 m/d. Starting from an initial state of zero solute concentration, the aquifer is gradually contaminated due to transport of solute from a line source of pollution at  $y = 0$  due to both advection and dispersion.

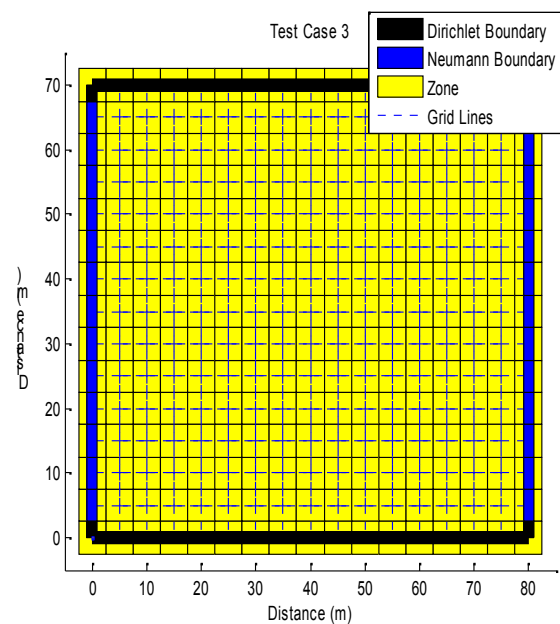


**Figure 1** Schematic of aquifer modeled in Test Case for the simulation of solute transport in uniform one dimensional groundwater flow in unconfined aquifer under the line source of pollution conditions

For solute transport simulations by RWSOLUTE and MMOC SOLUTE models, the aquifer is discretized by using a mesh-centered finite difference grid. The nodal spacing in x- and y- direction is kept uniform as 5 m. The total nodes in the finite difference grid are 255 while the total boundary nodes are 60. For solute transport simulation by FESO-

LUTE model, a triangular finite element mesh is used with isosceles triangular elements of size 5 m resulting into 448 finite elements. The aquifer parameters used in this test simulation are aquifer thickness ( $b=30$  m), effective porosity ( $\theta=0.30$ ), transmissivity ( $T=10$  m<sup>2</sup>/d), specific yield ( $S_y=0.10$ ) and longitudinal dispersivity along y-direction ( $\alpha_L=10$  m).

**Validation of FESOLUTE, MMOC SOLUTE & RWSOLUTE models**

Figure 2 shows transverse concentration profiles at  $y = 0$  from the analytical solutions and FESOLUTE, MMOC SOLUTE, and RWSOLUTE simulations. It is found from the comparison of the concentration profiles obtained from solute transport simulation models that the initial error in numerical solutions dampens out as the solution progresses through the time. Since both the MMOC SOLUTE and RWSOLUTE models use same discretization and the same interpolation schemes, better accuracy delivered by MMOC SOLUTE model can be attributed to the spatial decoupling resulting in smaller matrices to be solved. The RWSOLUTE concentration profile shows numerical overshoots at early times and deviate leftwards from the analytical concentration profile at later times. At distance of 10 m from the line source of pollution, the percentages of the deviation between MMOC SOLUTE and RWSOLUTE and analytical solutions are 5% and 30 % respectively.

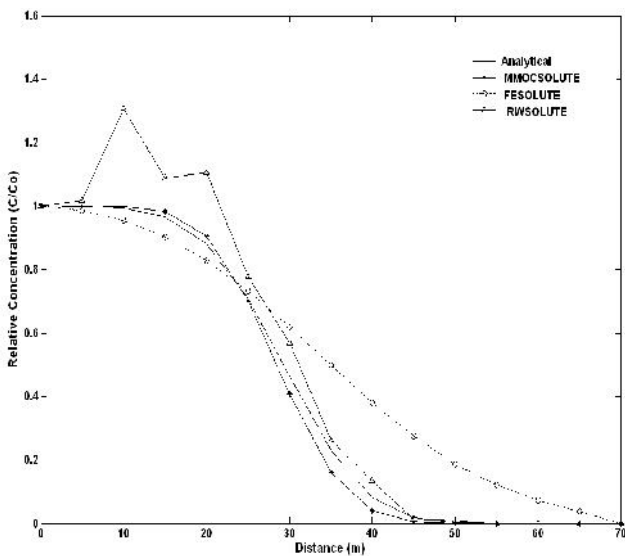


**Figure 2** Validation of FESOLUTE, RWSOLUTE and MMOC SOLUTE models for Test Case

**Comparison of mass balance error in FESOLUTE, RWSOLUTE & MMOC SOLUTE models**

Figure 3 shows the comparison of the total mass balance error in FESOLUTE, MMOC SOLUTE and RWSOLUTE model solutions. The rise in mass balance

curve is very sharp in the early stages of the simulation up to 3 days. Thereafter the mass balance error curves increase gradually till the end of the simulation period of 30 days. It is found from the results that the mass balance error curve of RWSOLUTE and FESOLUTE simulations deviate from MMOC SOLUTE simulations by an order of 34% and 2.54% respectively. Thus the MMOC SOLUTE simulations are found to be more accurate than the remaining two models. The RWSOLUTE simulations are more erroneous because of the randomness in generation of the particles to simulate the solute transport process. The FESOLUTE simulations are less accurate as compared to MMOC SOLUTE simulations because of the lower order basis function used in the finite element formulation. As the simulation progresses the numerical oscillations get dampened and consequently the errors in the later stages of the simulation are comparatively less than the error in early stages of the simulation. However the presently chosen MMOC method gives an acceptable much lower error, whereas random walk is more approximate in dealing with hydrodynamic dispersion.

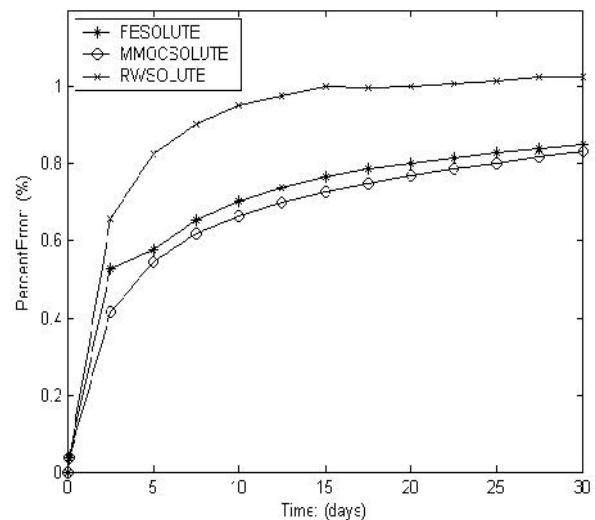


**Figure 3** Comparison of mass balance errors in FESOLUTE, MMOC SOLUTE and RWSOLUTE models for Test Case

**Effect of time step size on FESOLUTE, MMOC SOLUTE & RWSOLUTE solutions**

Figures 4.18 shows the transverse concentration profiles at  $y = 0$  obtained by FESOLUTE model, for the 0.125-day, 1.25-days, and 3.75-days time step simulations. It is found that the simulation results from a tenfold increase in time step size from 0.125-day to 1.25-days match closely. However when thirty fold increase in time step that is 3.75 days is experimented, the simulation shows numerical dispersion. The relative concentration of 0.5 is observed at 33 m and 32 m distance from the source of pollution for 0.125-day and 1.25-days time step simulations. With the uniform velocity of 1.0 m/d in y-direction and 1.0 m<sup>2</sup>/d of dispersion coefficient, the relative concentration of 0.5 is expected at 35 m distance from the source of the pollution. But the leftward deviation of the concentration profiles is due to the numerical dispersion which is 5.71% and 8.57% for the concentra-

tion profiles for 0.125-day and 1.25-days time step simulations. The numerical dispersion noticed in the concentration profile obtained for 3.75-days time step size simulation is 31%. The overshoot in the numerical solution due to a large time step size of 3.75-days is observed to be around 35 % in the close vicinity of pollution source. It is seen from the Figure 4.19 that the RWSOLUTE simulated concentration profiles for the 3.75-days time step size are severely affected by numerical oscillations and dispersions. The solutions are found to be reasonably accurate for the time step size of 0.125-day. Even for the choice of time step size of 1.25-days, an overshoot in the numerical solutions of around 30% is observed at 10 m downstream from the line source of pollution.

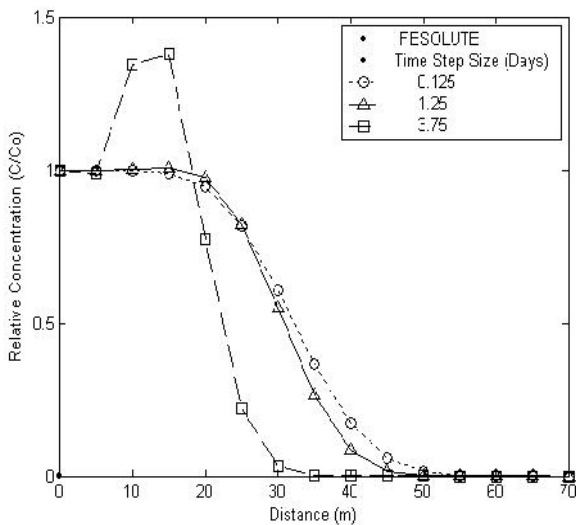


**Figure 4** Effect of time step size on FESOLUTE model solutions for Test Case

The unacceptable overshoot of 100 % is noticed at the distance of 25 m downstream of the source for 3.75-days time step simulation. Thus the RWSOLUTE simulations are found to be severely restricted by the choice of time step size. When using MMOC SOLUTE modeling, it is observed from the Figure 4 that at 35 m downstream of the source the relative concentrations are 0.43, 0.40, and 0.16 for 0.125-day, 1.25-day, and 3.75-days time step size simulations, respectively. Thus the numerical dispersion of 34% is noticed for the 3.75 days time step simulation. But there is an absence of numerical oscillation in all the concentration profiles simulated with 0.125 and 1.25-days simulation. This shows better performance of the MMOC based solute transport model.

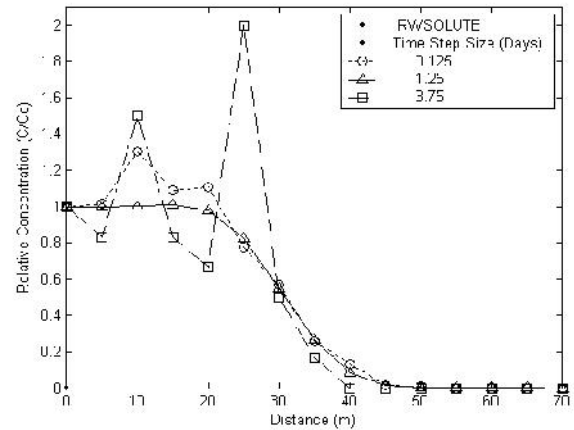


**Figure 5** Effect of time step size on model RWSOLUTE solutions for Test Case

**Effect of particle mass on RWSOLUTE solutions**

Figure 6 shows the effect of particle mass variation on the shape of the concentration profiles simulated by RWSOLUTE model. The fixed particle mass signifies the fraction of the total solute mass residing in the unit volume of groundwater at a given point of time. The particle mass is a fixed quantity while the number of particles is only varying due to the transport of the solute mass in a given time step. The particle mass is varied from 1.0 gm to 10.0 gm. The numerical solutions experienced oscillations up to the distance of 20 m from the source of the pollution for all the chosen values of the particle mass. The maximum overshoot is observed in the concentration profile simulated for the 10.0 gm particle mass to the order of 50% and the maximum undershoot is found in the concentration profile simulated for 5.0 gm particle mass which is of the order of 30%.

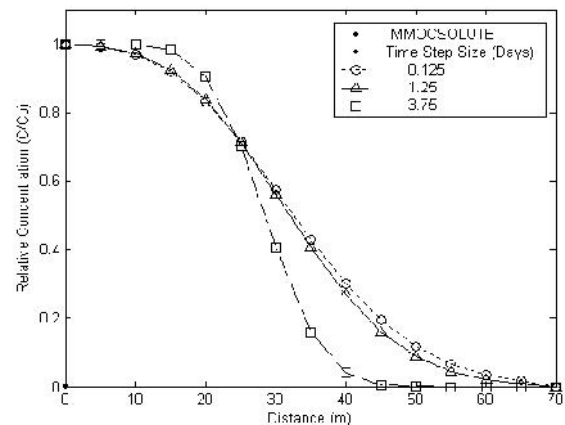


**Figure 6** Effect of time step size on MMOC SOLUTE model solutions for Test Case

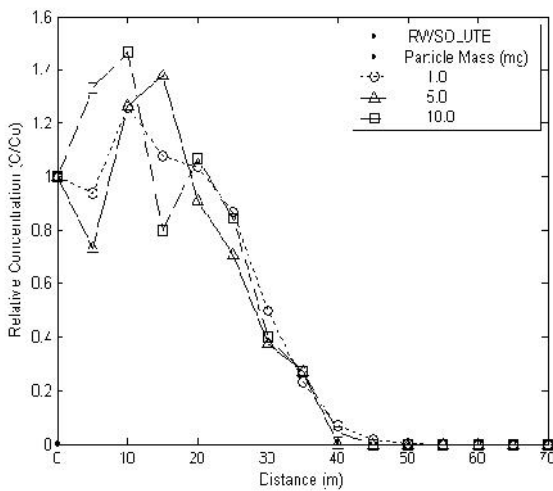


**Figure 7** Effect of particle mass on RWSOLUTE model solutions for Test Case

For the particle mass of 1.0 gm the relative concentration of 0.5 at the distance of 30 m downstream of the source location and the corresponding numerical dispersion is 14%. The reduction in numerical oscillations for fewer particles mass can be attributed to the large number of particles used in the simulation. If the particle mass is less it means that large number of particles are used in solute transport simulation which helps in better resolution of concentration fronts in the close vicinity of the source of the pollution.

### VIII. CONCLUSIONS

The conclusions from this present study are given as:

Validation of FESOLUTE, RWSOLUTE and MMOC-SOLUTE for chosen Test Case show that the numerical dispersion in solute concentration profiles obtained by MMOC-SOLUTE, FECSOLUTE and RWSOLUTE models are 2%, 4% and 24% respectively.

The investigations pertaining to the effect of time step size (Courant number) on proposed transport models reveal that MMOC-SOLUTE and FESOLUTE produce stable results for the time step size of 0.125 days while the RWSOLUTE solutions suffer from high overshoots in the solutions to the order of 28% higher than analytical solutions even for smaller time step of 0.25 day

RWSOLUTE model produces 20% higher mass balance error compared to the other two models. The average mass balance error in MMOC-SOLUTE model is less than the remaining two models, thereby proving it as a better performing model. MMOC-SOLUTE model provides better accuracy as compared to other two models by controlling the numerical dispersion through adequate treatment of the hydrodynamic dispersion term. The results of RWSOLUTE simulations show that the numerical undershoot and overshoot in solute concentration profiles are of two orders magnitude greater than MMOC-SOLUTE model. It is found that in MMOC-SOLUTE model adequate treatment of dis-

persion term helps in controlling the numerical dispersion as compared to FESOLUTE model. Therefore the above numerical experiments encouraged the author for the application of MMOC-SOLUTE model for field application.

It is also found that the RWSOLUTE solutions are sensitive to the choice of particle mass and in turn to the number of particles generated to represent the solute mass in aquifer system. Study noted that almost all model solutions develop numerical oscillations with the increase in time step size. It is found from the RWSOLUTE simulations that large mass balance errors up to 25% may occur when less number of particles is used in the solute transport simulation.

### IX. REFERENCES

- [1] Garder, A. O., Peaceman, D. W., and Pozzi, A. L. Jr., 1964, Numerical calculation of multidimensional miscible displacement by the method of characteristics, *Society of Petroleum Engineers Journal*, 4(1):26-36.
- [2] Bredeheoft, D., and Pinder, G. F., 1973, Mass transport in flowing groundwater, *Water Resources Research*, 9(1): 194-210.
- [3] Smith, I. M., Farraday, R. V., and O'Connor, B. A., 1973, Rayleigh-Ritz and Galerkin finite element for diffusion-convection problems, *Water Resources Research*, 9(3):593-605.
- [4] Freeze, R. A., and Cherry, J. A., 1979, *Groundwater*, Prentice-Hall, Englewood Cliffs, New Jersey.
- [5] Neuman, S. P., 1984, Adaptive Eulerian-Lagrangian finite element method for advection-dispersion, *International Journal of Numerical Methods in Engg.*, 20: 321-337.
- [6] Sorek, S., 1988, Eulerian-Lagrangian method for solving transport in aquifers, *Advances in Water Resources*, 11: 67-73.
- [7] Uffink, G. J. M., 1988, Modeling of solute transport with the random walk method, Proceedings of International Conference on Groundwater Flow and Quality Modelling (Eds. E. Custodio et al.), D. Reidel Publishing Company, The Netherlands: 247-265.
- [8] Illangasekare, T. H., and Doll, P., 1989, A discrete kernel method of characteristics model of solute transport in water table aquifers, *Water Resources Research*, 25(5): 857-867.
- [9] Sun, N.-Z., 1996, *Mathematical Modeling of Groundwater Pollution*, Kluwer Academic Publishers, Netherlands.
- [10] Wen, X. -H., and Hernandez, J. J. G., 1996, The constant displacement scheme for tracking particles in heterogeneous aquifers, *Ground Water*, 34(1):135-142.